ATLAS NOTE

August 6, 2021

Search for displaced diphoton resonances with the ATLAS detector in $\sqrt{s} = 13\ TeV$ pp collisions

Suchitoto Rose Tabares-Tarquinio
University of San Francisco
REU Program at Nevis Laboratories

Abstract

This paper outlines the analysis searching for displaced diphoton resonances originating from the decay of a long-lived particle. A number of leading theories of physics beyond the Standard Model suggest the existence of partner sparticles for every particle in the SM. This paper analyzes the pair production of long-lived Higgsinos (sparticles of the Higgs) Gauge Mediated Supersymmetry Breaking signal model to predict long-lived particles of their children decaying resonantly to 2 photons: Hyy. Because the final state electromagnetic objects share the same parent, the combined detector information of the two photons can be used to determine their production vertex, revealing information about the lifetime of the parent higgsino. The similarity of photons to electrons at high displacement motivates the inclusion of a di-electron vertex signal, where the parent particle is a Z boson instead of a Higgs: Zee. The analysis makes use of a novel trackless calo-vertexing method, which uses calorimeter pointing and timing information to determine the vertex displacement of a di-eλ resonance. The search is performed on the full Run 2 ATLAS dataset, corresponding to 139fb $^{-1}$ of pp collisions with a center-of-mass energy of $\sqrt{s} = 13\ TeV$.

Contents

1 Introduction **3**
1.1 The Standard Model of Particle Physics and the Higgs Boson 3
1.2 Supersymmetry 4
1.3 The Large Hadron Collider and ATLAS 5

2 Search for Displaced Diphoton Resonances **6**
2.1 Displaces Diphoton Resonances 6
2.2 Trackless calo-vertexing method 8

3 Data and Monte Carlo Simulations **9**

4 Preselections and Cuts **10**
4.1 Basic cuts 10
4.2 Trigger 10
4.3 Detector Region 10

5 Analysis and Optimization **11**
5.1 Timing and Vertexing by Photon Identification 11
5.2 Validation Region Signal Contamination Study 15

6 Conclusion and Next Steps **17**

Acknowledgements **17**

References **18**

1 Introduction

1.1 The Standard Model of Particle Physics and the Higgs Boson

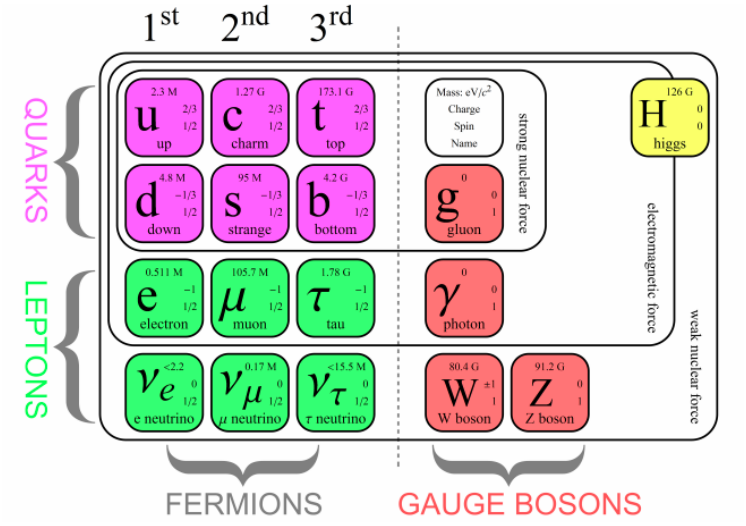

Figure 1: Credit: Matic Lubej, University of Ljubljana

The Standard Model (SM) is a quantum field theory (QFT) that describes three of the four fundamental forces in the universe and classifies most known elementary particles. Elementary particles are broken down into three basic groups: fermions, gauge bosons, and the Higgs boson.

Fermions are half integral spin particles that bind together to form matter, acting as the building blocks of non-fundamental particles: quarks, which make up protons and neutrons; and leptons, which include electrons, muons and neutrinos. Both quarks and leptons are further subdivided into three generations, or flavors.

Gauge bosons are force carriers that mediate the interactions between the fermions. Different types of bosons carry different fundamental forces. Photons, which carry the electromagnetic force, tying electrons to their nuclei or binding atoms into molecules and Gluons, which carry the strong force which operates only on quarks, particles which maintain a color charge, and binds them together to form protons and neutrons, both massless. W and Z bosons, which carry the weak force, have mass.

The Higgs boson is not a gauge boson but instead mediates particles' interaction with the Higgs Field, which is responsible for giving other particles the ability to gain mass through the Brout-Englert-Higgs mechanism. The Higgs boson was discovered in 2012 by CERN in the mass region around 125 GeV and in 2013 Englert and Higgs were awarded the Nobel Prize.

Other types of Higgs bosons are predicted by other theories that go beyond the Standard Model.

1.2 Supersymmetry

The Standard Model predictions have been substantiated by experiments over decades, with the most recent such confirmation in the 2012 discovery of the Higgs boson by the ATLAS and CMS Experiments at CERN. In spite of these successes, the absence of an SM explanation for the last fundamental force: gravity, and its corresponding elementary particle: the graviton, for dark matter, for the observed physical Higgs mass, and many other key phenomena all point to the need for new fundamental physics just above the weak scale: Beyond the Standard Model physics.

Supersymmetry (SUSY) is a well-motivated theoretical extension to the SM. The theory introduces the existence of partner sparticles for every particle in the SM in a flexible framework with many free parameters. In many formulations of SUSY, these sparticle partners exist at the TeV scale and thus can be accessible at the LHC. As a result, the ATLAS and CMS experiments have broad search programs for these sparticles.

Supersymmetry takes all particles in the Standard Model and gives them a superpartner that differs by spin ½ (fermions become bosons and vice versa). So far, it is believed that Dark Matter can be accounted for by a particle that is either stable, or has a lifetime much larger than that of the universe. This requirement can be achieved by an appropriate symmetry imposed on SUSY. An exact discrete Z2 symmetry of SUSY, called R-parity, gives a stable Lightest Supersymmetric Particle (LSP) which could, if it weakly interacts with the other particles, be a viable Dark Matter Particle. The "higgsino" would be the super-partner of the Higgs boson.

The hierarchy problem is one of the naturalness problems of the Higgs sector in the SM. In the SM, the Higgs mass receives contribution from one-loop radiative corrections. This contribution is proportional to the square of the momentum running in the loop and can be set to the cut-off scale or larger than that. With the cut-off scale of the order of the GUT scale, $M_G \approx 10^{16}$GeV, Higgs mass is not protected to be of O(100 GeV) to break the electroweak symmetry.

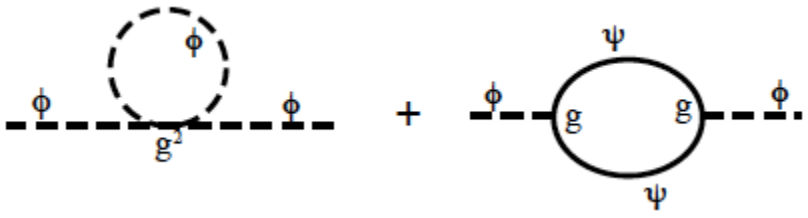

Figure 2: One loop diagrams which yield a corrections to the scalar mass

In SUSY, the loop diagrams, shown in Fig.2, that are quadratically divergent cancel, term by term against the equivalent diagrams involving superpartners:

$$m_h^2 = m_{h,tree}^2 + c\frac{g^2}{4\pi^2}M_{pl}^2, \qquad without\ SUSY$$
$$m_h^2 = m_{h,tree}^2\left(1 + c'\frac{g^2}{4\pi^2}\ln\left(\frac{M_{pl}}{M_W}\right)\right) \qquad with\ SUSY$$

Figure 3: Observable Higgs mass equations with and without SUSY

1.3 The Large Hadron Collider and ATLAS

The Large Hadron Collider (LHC) at the European Organization for Nuclear Research (CERN) is the world's largest and most powerful particle accelerator. Located underground near Geneva, Switzerland, the facility consists of a 27-kilometer ring of superconducting magnets with accelerating structures to boost the energy of the particles as they travel in opposite directions to nearly the speed of light colliding at rates up to 40 MHz and center-of-mass energies up to 13 TeV. Proton-proton and heavy-ion collisions delivered by the LHC recreate the conditions immediately following the Big Bang, and allow ATLAS to investigate fundamental questions such as the Brout-Englert-Higgs field or Dark Matter. ATLAS also studies the elementary subatomic particles of the Standard Model (SM) to determine if they are indeed elementary. Possible discoveries at the LHC could validate models, such as those incorporating Supersymmetry (SUSY), where the fundamental forces unify at very high energies.

Figure 4: A view of the LHC with the locations of various experiments labelled.

The ATLAS (A Toroidal LHC ApparatuS) experiment at CERN is one of several international collaborations that conduct research at the LHC. The ATLAS detector consists of an inner tracking detector surrounded by a thin superconducting solenoid providing a 2 Tesla axial magnetic field, electromagnetic and hadronic calorimeters, and a muon spectrometer. Lead/Liquid-Argon (LAr) sampling calorimeters provide electromagnetic (EM) energy measurements with high granularity. The endcap and forward regions are instrumented with LAr calorimeters for both the EM and hadronic energy measurements up to |eta | = 4.9. The ATLAS

detector uses a number of rapid triggering systems to filter the large amount of data generated. Once data is stored, signatures from the detector are characterized and analyzed around the world.

The Liquid-Argon (LAr) calorimeter electromagnetic (EM) performance is particularly important for this analysis, which seeks to identify signal photons that do not point back to the primary vertex and that reach the calorimeter after some delay.

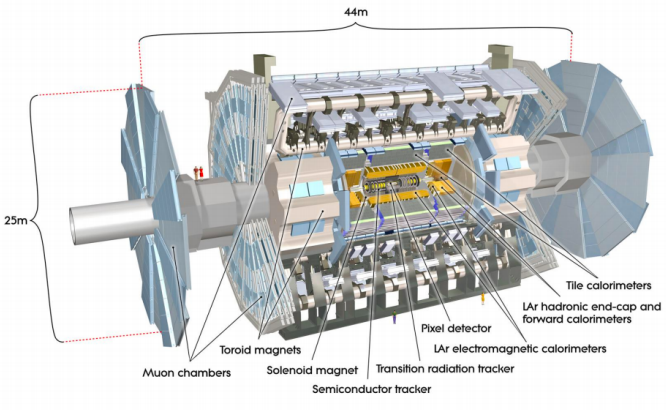

Figure 5: ATLAS detector, Credit: CERN

2 Search for Displaced Diphoton Resonances

2.1 Displaces Diphoton Resonances

Of the many new particles predicted in SUSY, sensitivity and therefore mass exclusions are generally weakest for supersymmetric electroweak bosons (electroweakinos), due to their low production cross sections in proton collisions and decays that are kinematically similar to SM background processes.

This search focuses on a specific set of SUSY models with Gauge Mediated Supersymmetry Breaking (GMSB), which have some notable distinctions from the nominal paradigm. Specifically, the ninoone is unstable and dominantly decays to an electroweak boson and a gravitino lightest supersymmetric particle (LSP), which can only be measured as contributing to MET (Missing Transverse Energy/momentum). The lifetime of these particles is a free parameter in the model, and most dedicated electroweak SUSY searches so far only consider prompt electroweakino decays. Combining the GMSB phenomenology with the relatively weaker limits on electroweak SUSY and the absence of results for long lifetimes leads to the signal pursued in this analysis.

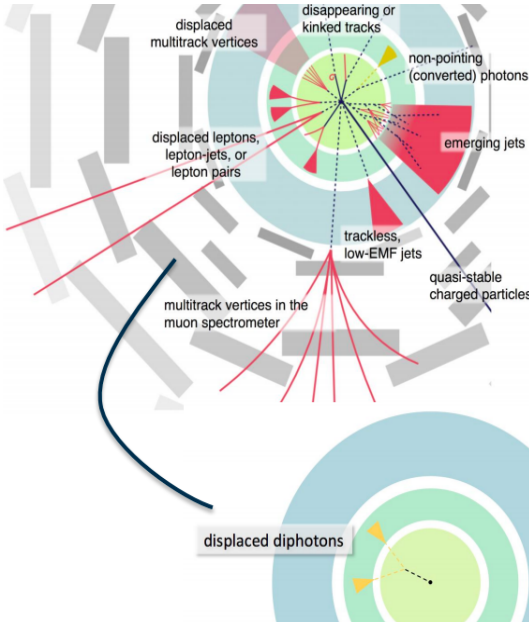

Figure 6: Displaced diphoton resonances originating from the decay of a long-lived particle.

We perform a search for direct pair production of Long-Lived electroweakinos in a GMSB signal model that predicts Long-Lived Particles (LLP) decaying to a Higgs boson and a gravitino, with the Higgs subsequently decaying resonantly to 2 photons. The similarity of photons to electrons at high displacement motivates the inclusion of a di-electron vertex signal, where the parent particle is a Z^0boson decaying to two electrons.

Because the final state EM objects share the same parent, the combined detector information of the two photons/electrons can be used to determine their production vertex, revealing information about the lifetime of the parent higgsino.

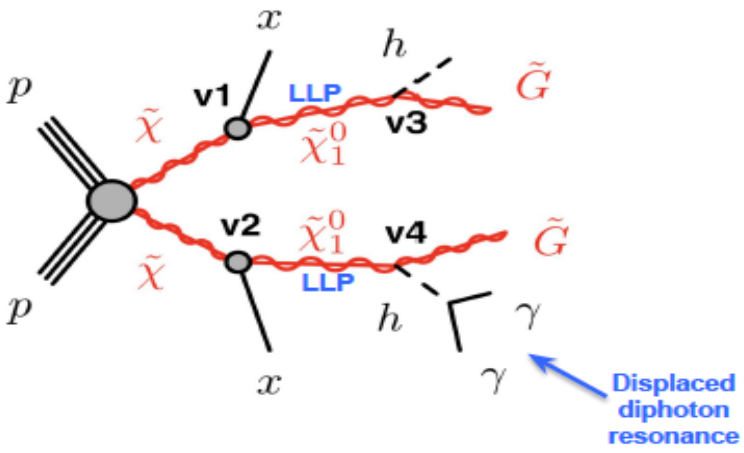

Figure 7: A Feynman diagram of the signal studied in this analysis, which shows the direct pair production of neutralinos decaying to a final state of two Standard Model Higgs bosons and two gravitinos. This shows when only Higgs decays to two photons are considered.

2.2 Trackless calo-vertexing method

The analysis makes use of a novel trackless calo-vertexing method, which uses calorimeter pointing and timing information to determine the vertex displacement of a di-EM resonance. This method is approximately equally performant for both photons and electrons, opening up the decays that can be considered in the analysis.

Being track-agnostic (trackless) recovers the loss in efficiency by requiring a track, which drops as a function of displacement. This technique therefore is more sensitive to longer lifetimes (ct) than searches that depend on large radius tracking, which covers vertices only up to ~300 mm displacement in the transverse plane. Calo-Vertexing finds the displaced vertices using only LAr measurements by using photon pointing and LAr Timing information.

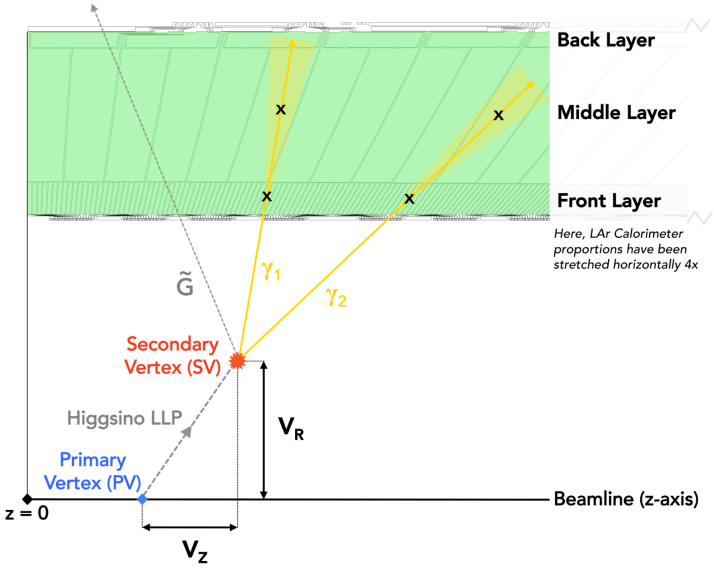

Figure 8: LAr Vertexing

Photon pointing refers to the position on the z-axis where the photon "points" back to which is measured by drawing a line through two points: LAr cells are finely segmented in η, which allows for precise photon pointing measurements. However, they are coarsely segmented in φ, which proves to be the greatest hurdle in 3D calo-vertexing. Due to poor phi resolution, which "contaminates" our vertex in 3D, we choose to ignore phi measurements and still obtain two-dimensional (2D) vertex information. This 2D vertexing procedure is constructed by projecting all photon measurements onto the R-Z plane (slice phi=0), draw a line through the photon shower barycenters in the front and middle layers of the LAr calorimeter, and find the point of intersection of these two lines defined as the vertex position. Secondary vertex reconstruction requires precise information from the LAr calorimeter to measure each photon's direction and timing. The ATLAS group at Columbia University has great expertise in the electromagnetic LAr calorimeter of the ATLAS detector which gives them perfect insight into studying the Higgsino and long-lived particles.

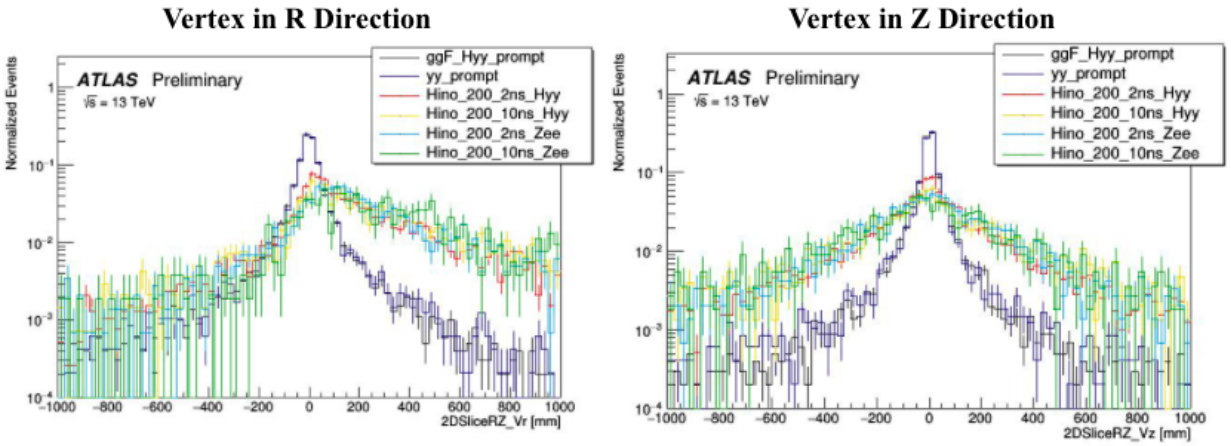

Figure 9: Reconstructed Vertex in R (left) and in Z (right).

3 Data and Monte Carlo Simulations

In this study we used background data in conjunction with simulated long-lived Higgsino signals Background data taken by the ATLAS experiment during a 2015-2018 run at the LHC. The signal grid is defined by the neutralino mass and lifetime. In order to focus on the decays that can be detected by trackless calo-vertexing, generated events are filtered such that only **Hyy** and **Zee** final states are included. Since the long-lived neutralinos are pair-produced, each event will have two final state **H/Z^0** bosons. Only one is required to decay to the desired di-EM resonance, and the other takes its SM branching ratios. Therefore, four signals are generated for each point in the mass/lifetime grid: Hyy+H->SM, Hyy+Z->SM, Zee+H->SM, and Zee+Z->SM. Because the branching ratio and thus yields for the Zee final state points are much higher than the **Hyy**, only **Zee** final states are sensitive for the highest neutralino masses. The privately produced long-lived Higgsino samples (NTuples and MicroNTuples) generated 10-20k events for signal points covering timescales from 2-10 ns and mass scales from 100 –800 GeV. A summary of the generated signal grid can be seen in Figure 10.

Higgsino Mass [GeV]	100	150	200	300	400	500	600	800	1000
Final State: HyyHSM		✓	✓	✓	✓	✓	✓		
Final State: HyyZSM		✓	✓	✓	✓	✓	✓		
Final State: ZeeHSM		✓	✓	✓	✓	✓	✓	✓	✓
Final State: ZeeZSM	✓	✓	✓	✓	✓	✓	✓	✓	✓

Generate each point with higgsino lifetimes of: **2 ns**, **10 ns**

Figure 10: Analysis signal grid, broken down by higgsino mass and lifetime, and final state. 2ns and 10ns are the benchmark lifetimes for the ongoing NPP analysis (glance). We can use a lifetime reweighting procedure to extrapolate intermediate lifetimes. Because not all events are weighted equally with data, the weight of every single event is equal to 1, but our Monte Carlo signal samples have a better ratio so weight is much less than 1.

4 Preselections and Cuts

Photon objects in the analysis are subject to a basic preselection. At least two photons are required in the event.

4.1 Basic cuts

Photon pT > 35/25 GeV. Absolute value of both leading and subleading photon timing less than 12ns: abs(ph1_t) < 12 && abs(ph2_t) < 12. Reconstructed vertex in R < 1050 mm and reconstructed vertex in Z < 3000 mm. Eta separation between photon pointings greater than 0.1: abs(dEta_ph) > 0.1. Higs Candidate Mass between 60 and 160 GeV.

4.2 Trigger

Trigger is a system that uses simple criteria to rapidly decide which events to keep when only a small fraction of the total can be recorded. Several different triggers were considered to select the signal of interest. Given that the final state of the long-lived higgsino decay contains both two photons and missing energy from the gravitino, both diphoton and Missing Transverse Energy (MET) triggers were studied for maximal signal efficiency.

4.3 Detector Region

One photon must be in the barrel (|eta| < 1.37), while the other photon can be either in the barrel or the endcap (|eta| < 1.37 || 1.52 < |eta| < 2.37). The crack region of the calorimeter (1.37 leq|eta|leq 1.52) is excluded. Events that pass BB detector region selection have both photons in the barrel. Events that pass BE selection can be either of two cases: leading photon is in barrel and subleading photon is in endcap or vice versa (leading photon in endcap and subleading photon in barrel).

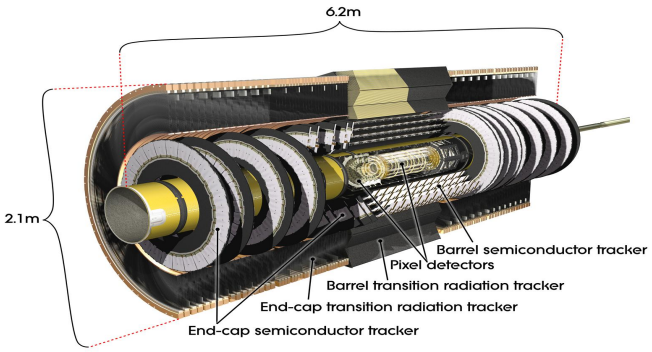

Figure 11: Atlas Inner Detector

In the following section, studies for determining the validation region cut and photon identification will be described.

5 Analysis and Optimization

5.1 Timing and Vertexing by Photon Identification

Tight ID means more strict requirements, therefore photons that pass Tight ID are almost certainly photons. However, reconstruction efficiency for real photons is lower than for other working points meaning you do not get all of the real photons. Loose ID means less strict requirements. Even though more objects will pass, you will get more of the real photons but you will also get fake photons (jets that have been reconstructed as photons).

The nature of non-pointing photons motivates careful choice of identification working point. The Tight ID working point imposes cuts on the shower shape variables, which are correlated to photon pointing and therefore introduce an undesired bias against non-pointing photons. The Medium selection only adds one additional cut to Loose, specifically on the photon shower shape variable known as E_ratio. Neither Medium nor Loose ID were found to introduce significant bias with pointing.

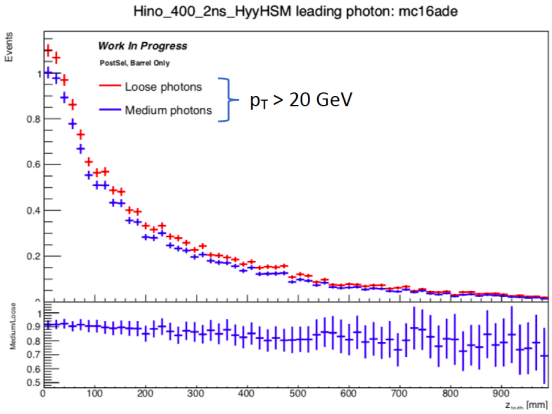

Figure 12: Ratio of Loose and Medium selected photons as a function of pointing

Furthermore, the use of Medium ID allows the analysis to take advantage of the lower trigger **pt** thresholds offered by the Medium diphoton triggers.

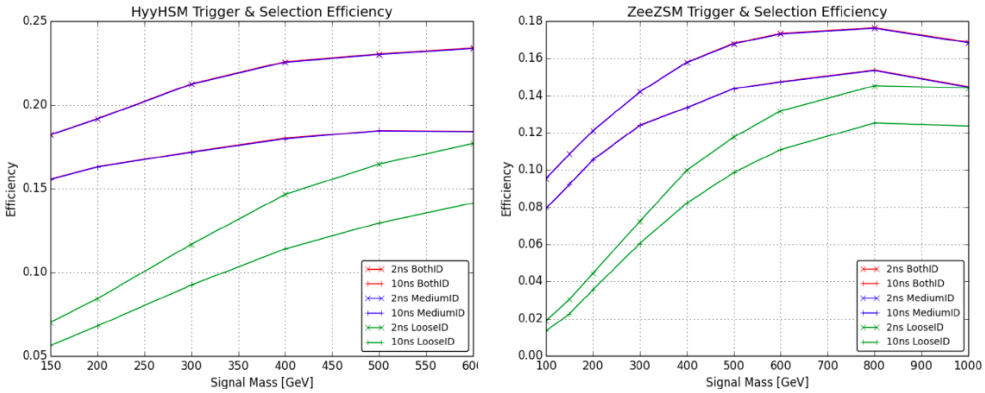

Figure 13: Loose Medium Efficiency

Therefore both photons are required to pass Medium ID requirements.

Displaced electrons are often reconstructed as loose photons, and loose photon triggers have been used to trigger on displaced electrons in the past. Most analyses use tight working points but because we are a long lived particle search, long-lived Higgsino, we have atypical photon objects. Since a long-lived Higgsino decays away from the primary vertex, when the photons hit the detector they do in an unusual angle, sometimes on an oblique angle, the tight working point is too stringent for our photon objects. All of our signals from our LLP demonstrate many of our photons will not pass the tight selection. Typically analysis will use tight photon ID because photons that pass tight ID are almost certainly photons, however reconstruction efficiency for real photons is lower than for other working points, therefore you do not get all of the real photons.

Real photons that are prompt in the data, have much narrower pointing, timing and vertexing distributions. We expect all photons in our control region to be prompt. But a jet that is identified as a photon will have a wider distribution. We want to quantify those distributions' shape differences as an uncertainty, to understand to what degree these distributions differ. We can compare real-enhanced and fake-enhanced categories. We define real-enhanced and fake-enhanced samples to understand what shape systematic we should apply.

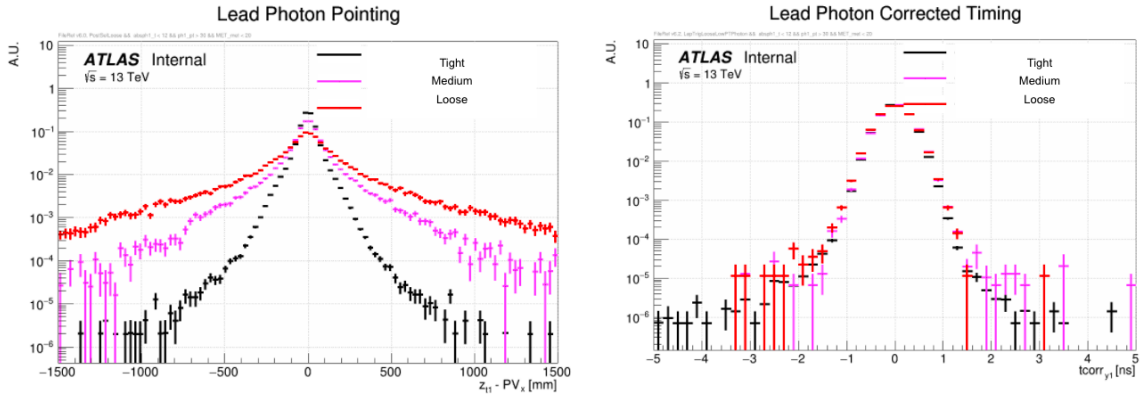

Figure 14: Lead photon pointing (left) shows how photons that pass tight ID have a much narrower shape distribution then photons that pass loose ID. Lead photon corrected timing (right) shows how photons that pass tight ID, medium ID, and loose ID have similar shape distribution.

For vertexing variables, we start with brute force plotting of the 9 orthogonal exclusive combinations of vertexing that encapsulate Loose, Medium, and Tight. We then reweighted CR distributions to the VR MaxEcell_E energy distribution.

Vertexing Combinations

		Photon 1		
		T	M && !T	L && !M
Photon 2	T	T T	M&&!T T	L&&!M T
	M && !T	T M&&!T	M&&!T M&&!T	L&&!M M&&!T
	L && !M	T L&&!M	M&&!T L&&!M	L&&!M L&&!M

Figure 15: 9 orthogonal exclusive vertexing combinations

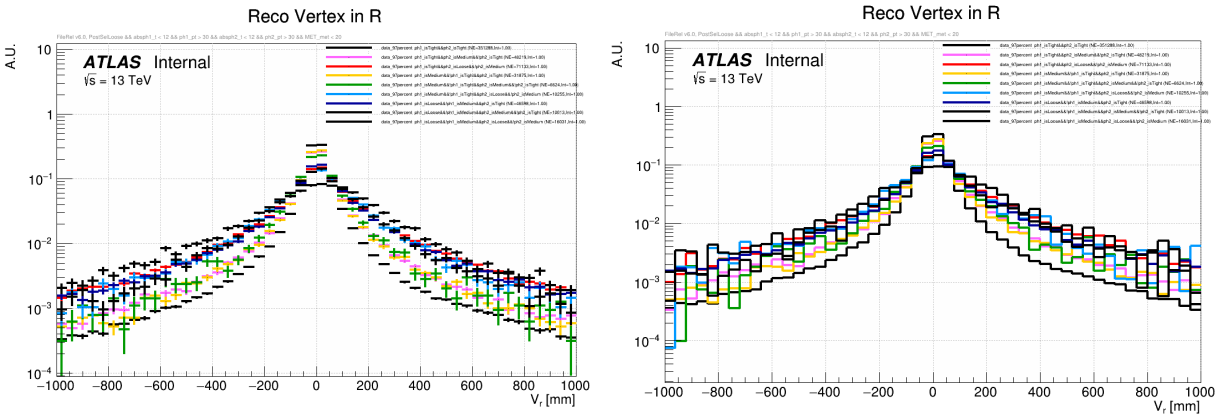

Figure 16: Reconstructed Vertex in R of the 9 vertexing combinations in (left). Same plot reweighted to VR MaxEcell_E energy distribution. More plots available here

From these plots we saw that some combinations have similar shape distributions and we decided to group them into four groups. Group one consists of both photons passing tight ID, in fig. 16 is the most narrow shape distribution black line and is the black line in fig. 18. Group two (red in fig. 17 and 18) consists of photon 1 medium photon 2 tight, photon 1 tight photon 2 mediu and both photons passing medium ID, in fig.16 is the green, pink, and yellow line and in fig. 18 is red line. Group three (yellow in fig. 17 and 18) consists of combinations where only one photon passes loose ID "single loose exclusive photon". Group four (pink in fig. 17 and 18) is the widest shape distribution, both photons passing loose ID.

Vertexing Combinations

Photon 2 \ Photon 1	T	M && !T	L && !M
T	T T	M&&!T T	L&&!M T
M && !T	T M&&!T	M&&!T M&&!T	L&&!M M&&!T
L && !M	T L&&!M	M&&!T L&&!M	L&&!M L&&!M

Figure 17: 9 orthogonal exclusive vertexing combinations grouped into four sub groups.

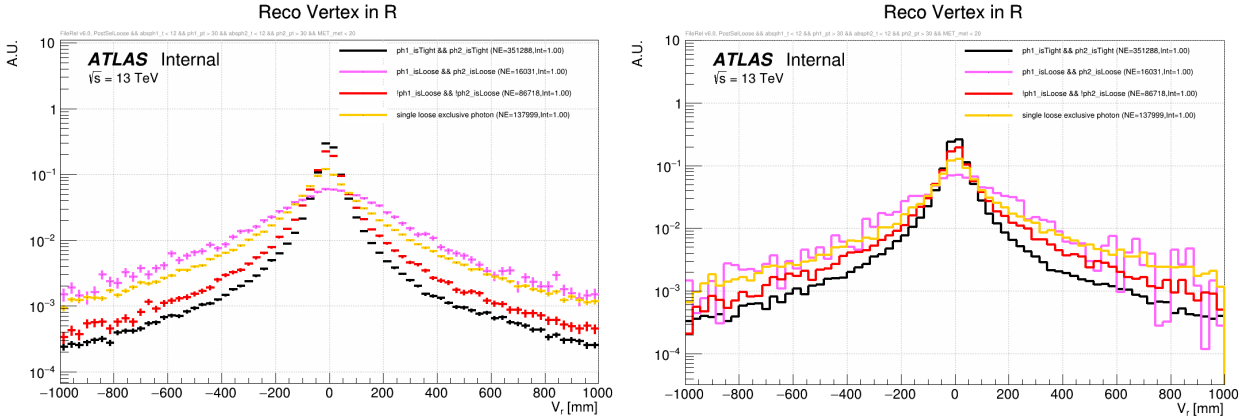

Figure 18: Reconstructed Vertex in R of the 4 vertexing combinations sub groups (left). Same plot reweighted to VR MaxEcell_E energy distribution. More plots

From these previous plots we saw that the shape distribution of the combinations that included a loose ID were too wide and did not contribute to the study, therefore we decided to drop loose ID (lines yellow and pink) and plot three groups: both photons pass tight ID (black line in fig. 19), exclusive medium (both photons pass medium ID but neither pass tight ID, pink line in fig. 19), and inclusive medium (only one also passes tight, red line in fig. 19).

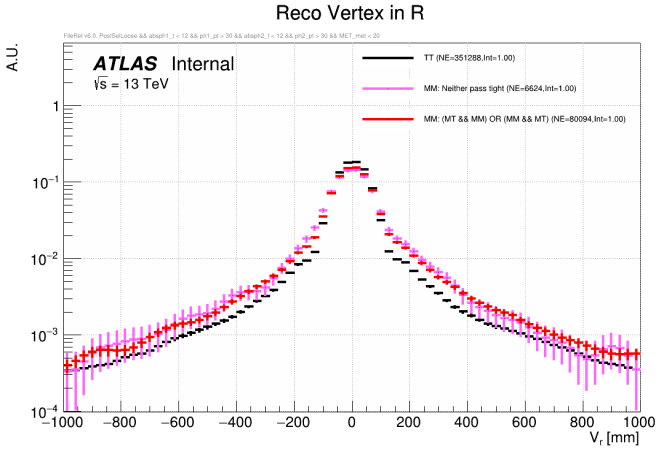

Figure 19: Reconstructed Vertex in R when dropping photons that pass loose ID. More plots

We then decided to group both medium sub groups (inclusive and exclusive) into one global medium group. We also decided to plot the total: sum of this global medium group and the tight group.

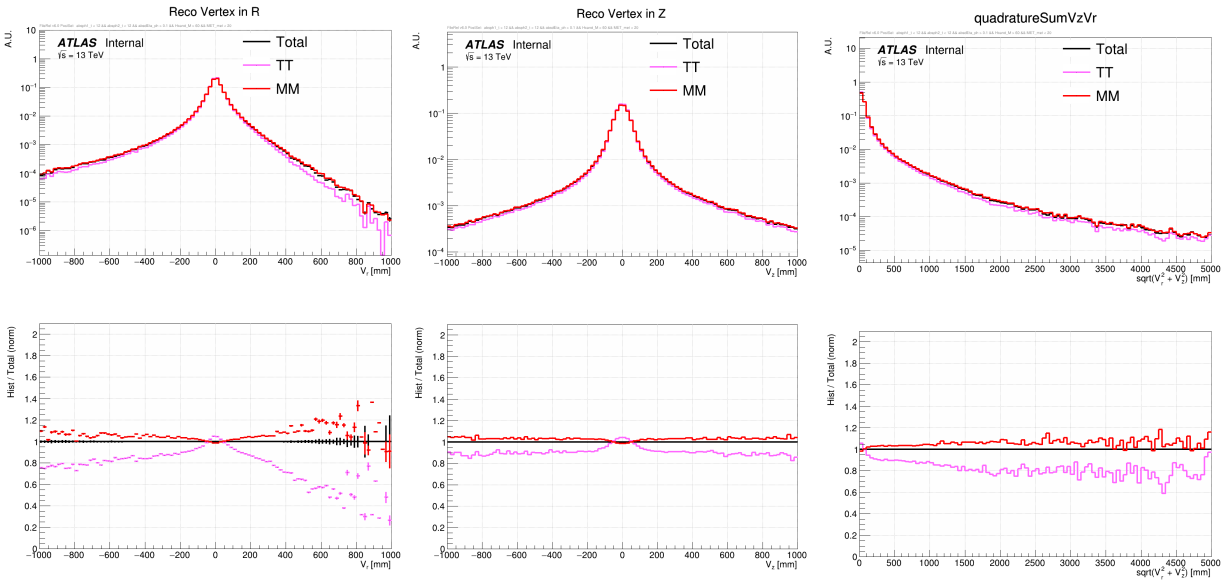

Figure 20: Reweighted CR distributions to the SR MaxEcell_E energy distributions Reconstructed Vertex in R comparing TT, MM (inclusive and exclusive), and Total (sum). More plots

5.2 Validation Region Signal Contamination Study

We choose our different analysis regions via MET (Missing Transverse Energy) since the MET in background data is much softer than MET in our signal Monte Carlo simulation. We like to have an intermediate Validation Region, where the background prediction can be checked.

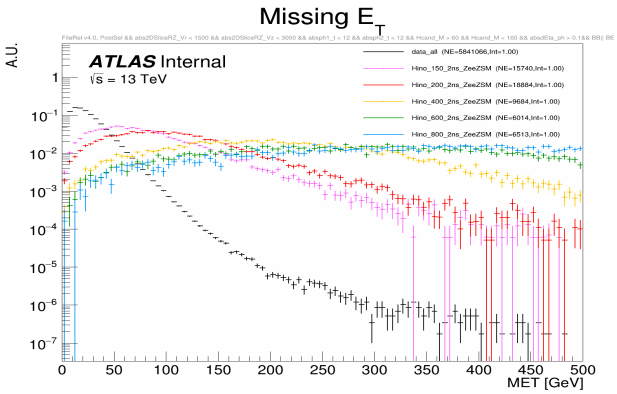

Figure 21: MET plot of background data (black line) and signal Monte Carlo simulations.

The Control Region (CR), is at low MET which produces a background-enriched region with negligible signal contamination. The Signal Region (SR), is at high MET which produces a signal-enriched region that drives the signal extraction but adds negligible constraints on the background parameters. This validation region signal contamination study aims to optimize the MET lower and upper cuts on the Validation Region (VR) to produce a region with enough events to give a good background estimation and has low signal contamination.

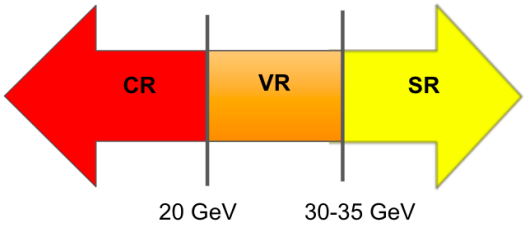

Figure 22: MET range for CR, VR, and SR region with proposed limits.

The cut we kept stable was the lower MET cut on the VR, requiring CR to be MET < 20 GeV and VR to be MET > 20 GeV. We then calculated the background yields and also signal contamination percentage of VR with an upper MET cut of 30 GeV and of 35 GeV for BB and BE regions to find which boundary limit optimizes the Validation Region.

To calculate the signal contamination percentage we took the ratio of signal event yields over data event yields and then turned into percentage: $Signal\ Contamination\ Percentage = 100 * \frac{Signal\ Event\ Yields}{Data\ Event\ Yields}$. We calculate event yields (for signal and for data it is the total number of events that we expect to get after some set of selections) and compare how many events we get in BB region vs BE region. Each region has different cuts for signal and data. PosPos means that both photons (ph1 “leading” and ph2

"subleading") have positive timing: ph1_t > 0 && ph2_t > 0. NegNeg means that both photons have negative timing: ph1_t < 0 && ph2_t < 0. For the Control Region we applied PosPos cuts for the signal and for the data. For the Validation Region and for the Signal Region we applied PosPos cuts for the signal and NegNeg cuts for the data, in order to keep the SR blinded until the analysis is finalized.

We calculated the data and signal yields and then from that calculated the signal contamination percentage of the validation region both with setting VR to be in the range of MET between 20GeV-30GeV and between 20GeV-35GeV. From the Data Yields 2D histograms (fig. 23), we see that a 35 GeV cut provides similar levels of background statistics (data yields) between the VR and SR and the 30 GeV cut has much less data yields in the VR region compared to the SR region. From the Signal Contamination Percentage 2D histograms (fig. 24) we see that a 30 GeV cut has lower signal contamination than a 35 GeV cut, which is what we are looking for. In conclusion, a 30 GeV cut provides lower signal contamination for all signal grid points and accomplishes such even while needing less data yields. Therefore, 30 GeV MET cut is the optimized boundary between VR and SR.

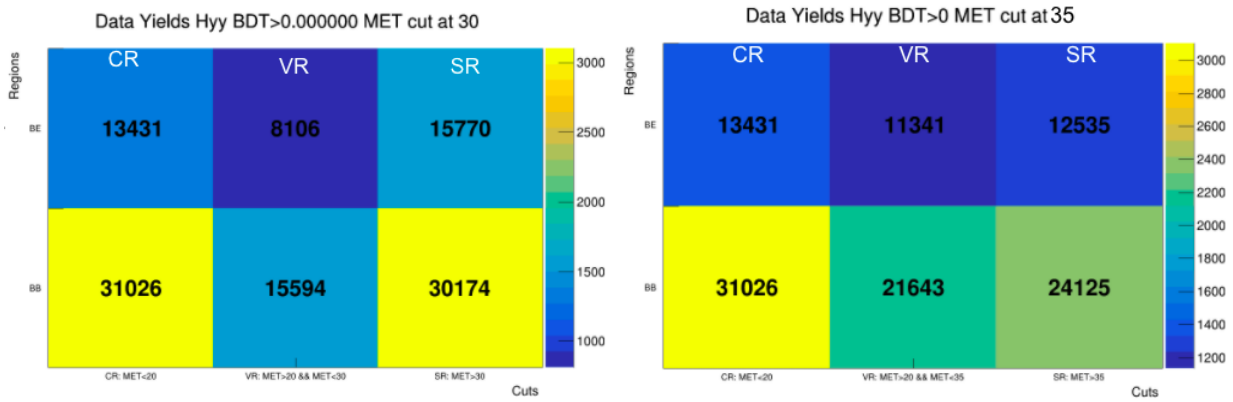

Figure 23: Data Yields 2D histograms with VR and SR boundary at 30 GeV (left) and at 35 GeV (right).

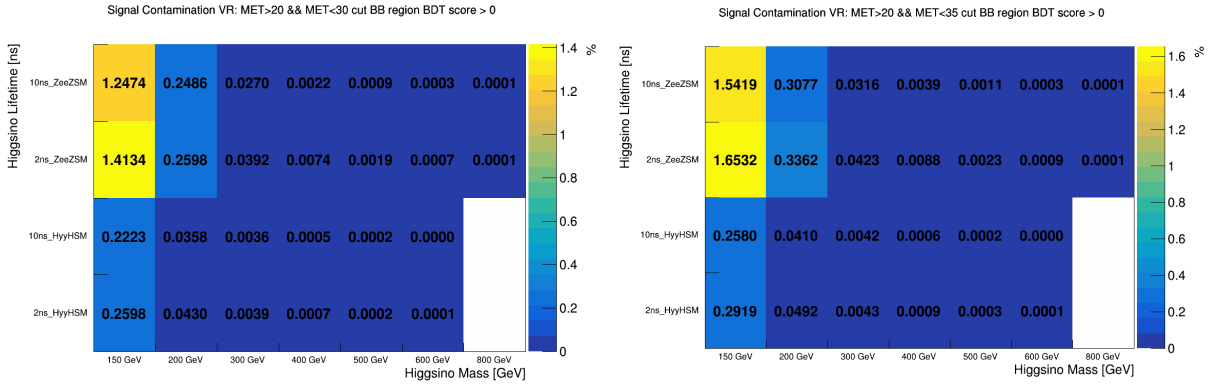

Figure 24: Signal Contamination Percentage of VR and SR boundary 30 GeV (left) and 35 GeV (right).

After deciding to set VR to be from 20 GeV to 30 GeV and therefore SR to be above 30 GeV, we also calculated the data and signal yields and the signal contamination percentage set at such MET ranges but now variating the Higgs Candidate Mass (Myy) cuts to determine if we

want to keep both limits: HCand_M > 60 GeV && HCand_M < 160 GeV, or if we want to drop the upper Myy cut and only limiting HCand_M to be greater than 60 GeV. From the Signal Contamination Percentage 2D histograms (fig. 25), we see that dropping the upper Myy cut produces lower signal contamination for all signal grid points. This study contributed to the decision to drop it, therefore only cutting at HCand_M > 60 GeV.

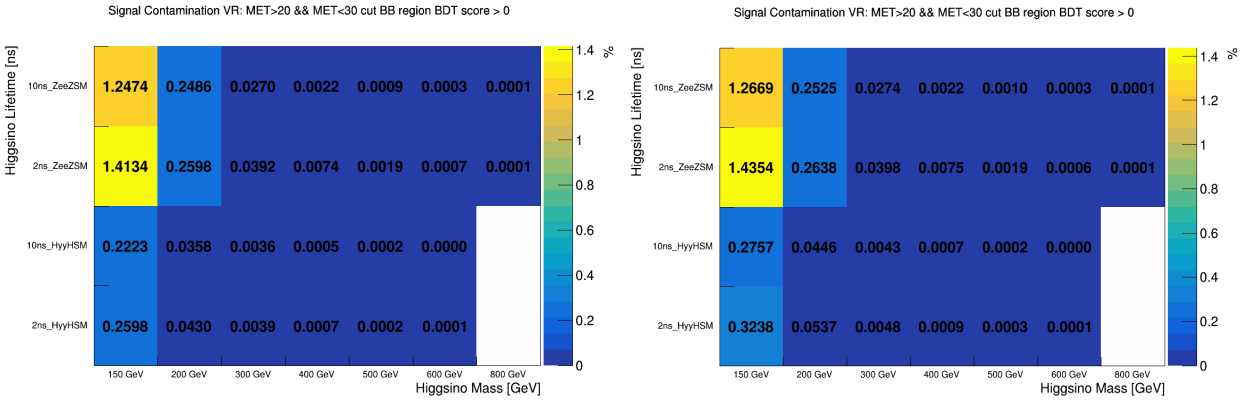

Figure 25: Signal Contamination Percentage 2D histograms when dropping upper Myy cut (left) and when having both limits (right). More plots

6 Conclusion and Next Steps

We are performing a trackless search for a displaced di-EM resonance. Benchmark model is a long-lived higgsino with a displaced H→yy or Z→ee. Sensitive variables include LAr Timing, and a novel Calo-Vertexing approach. The goal for my summer here at Nevis Laboratories ATLAS REU was to search for some optimized cuts that will help in the identification of displaced diphoton resonances. To do so I performed individualized studies such as the Timing and Vertexing by Photon Identification study and the Validation Region Signal Contamination helped find optimized cuts.

My signal contamination studies continue to inform the analysis strategy. I have made progress on the medium photon ID study, and will pass it along to someone else in the Columbia ATLAS team to be finalized.

Acknowledgements

First and foremost I would like to thank Kiley Kennedy for teaching me all about this analysis and for her help throughout this process. I would also like to thank Professor John Parsons for his mentorship and support throughout the REU program and working on this analysis. Another special thanks to Doctor Julia Gonski for her guidance. Many thanks as well to the National Science Foundation and Nevis Labs at Columbia University for the opportunity to do this research. This material is based upon work supported by the National Science Foundation under Grant No. PHY/1950431.

References

1. The ATLAS Collaboration (2014). Search for non-pointing and delayed photons in the diphoton and missing transverse momentum final state in 8 TeV pp collisions at the LHC using the ATLAS detector. *Atlas Publications*. Obtained from https://arxiv.org/abs/1409.5542

2. CERN. (2021). ATLAS Inner Detector. Obtained from https://atlas.cern/discover/detector/inner-detector

3. CERN. (2021). ATLAS Physics. Obtained from https://atlas.cern/discover/physics

4. https://home.cern/science/physics/supersymmetry

5. Displaced Diphoton Analysis internal note https://gitlab.cern.ch/atlas-physics-office/SUSY/ANA-SUSY-2020-28/ANA-SUSY-2020-28-INT1

6. Kennedy, K. (2020). Trackless Calo-Vertexing for Long-Lived Higgsinos with a Displaced Diphoton Final State. Obtained from https://indico.cern.ch/event/958400/contributions/4028833/attachments/2113902/3556198/LLHinoKickoff_KKennedy_10.01.20.pdf